

Rational design and regioselective synthesis of conformationally restricted furan-derived ligands as potential anti-malarial agents

Marius K. Mutorwa,^a Iviwe Nokalipa,^a Delia C. Tanner,^b Gregory L. Blatch,^{b,c}
Kevin A. Lobb,^{a,c} Rosalyn Klein,^{a,c} and Perry T. Kaye^{a,c} *

^aDepartment of Chemistry, ^bBiomedical Biotechnology Research Unit and Department of Biochemistry and Microbiology and ^cCentre for Chemo- and Biomedical Research, Rhodes University, Grahamstown, 6140, South Africa

E-mail: P.Kaye@ru.ac.za.

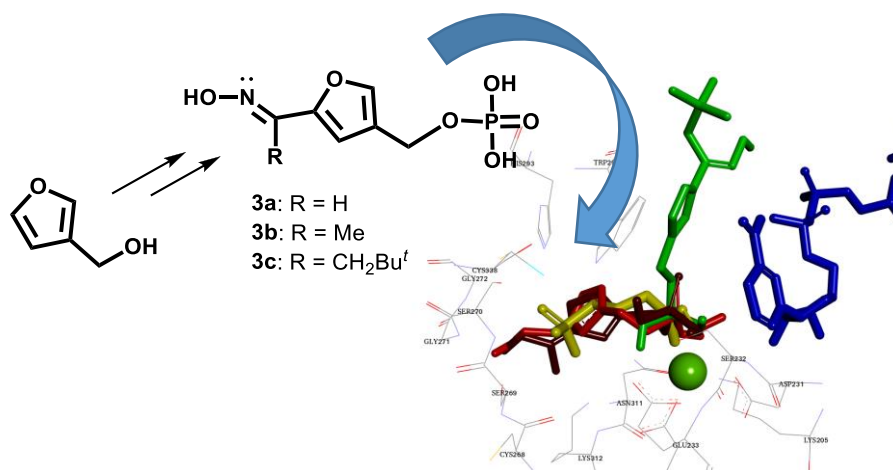
Received 06-30-2020

Accepted 01-23-2021

Published on line 02-05-2021

Abstract

Substituted 3-furanomethyl phosphate esters and their corresponding phosphoric acids have been prepared as conformationally restricted analogues of DOXP, the natural substrate for *Plasmodium falciparum* 1-deoxy-D-xylulose-5-phosphate reductoisomerase (*Pf*DXR), and fosmidomycin, an established inhibitor. Saturation Transfer Difference (STD) NMR analysis and *in silico* docking data suggest the potential of such compounds as *Pf*DXR inhibitors.



Keywords: Furan derivatives, 1-deoxy-D-xylulose-5-phosphate (DOXP), fosmidomycin, *Pf*DXR inhibitors, *in silico* docking, STD NMR.

Introduction

Malaria presents major and apparently continuing health challenges worldwide – particularly in Sub-Saharan Africa.¹ The situation is compounded by the emergence of drug-resistant *Plasmodium falciparum* (*Pf*) parasites,²⁻³ insecticide-resistant mosquitoes⁴ and the increased susceptibility to infection in HIV-positive individuals.⁵⁻⁷ Quinolines, anti-folates, hydroxynaphthoquinones, antibiotics and, latterly, artemisinins have all found use as anti-malarial agents.⁸ Artemisinin-based Combination Therapy (ACT),⁹ involving the use artemisinins (with short plasma half-lives) in combination with long-acting, anti-malarial drugs, has proved effective but expensive.

Various human pathogens,^{10,11} including *P. falciparum*, make exclusive use of the non-mevalonate 1-deoxy-D-xylulose-5-phosphate (DOXP)/2-C-methyl-D-erythritol-4-phosphate (MEP) pathway for the biosynthesis of isoprenoids. 1-Deoxy-D-xylulose-5-phosphate reductoisomerase (DXR), a key enzyme in this pathway, has been validated as a suitable target for therapeutic intervention,¹¹ and the antibiotic fosmidomycin **1** and its acetyl derivative FR900098^{11,13} have been shown to inhibit the enzyme. Numerous analogues of these compounds have been developed,¹⁴ and we have reported the synthesis and evaluation of phosphonated *N*-aryl- and *N*-heteroarylcarboxamides and (*N*-arylcabamoyl)alkylphosphonic acid derivatives^{15,16} as fosmidomycin analogues, *N*-substituted phosphoramidic acid esters as "reverse" fosmidomycin analogues¹⁷ and *N*-benzylated phosphoramidic acid derivatives as FR900098 analogues.¹⁸ Some approaches by other groups have focussed on the development of structural analogues of the natural substrate, DOXP **2**, as potential DXR inhibitors.¹⁹⁻²¹ We now report the regioselective synthesis of conformationally constrained furan-derived ligands, which incorporate structural features of both DOXP and fosmidomycin.

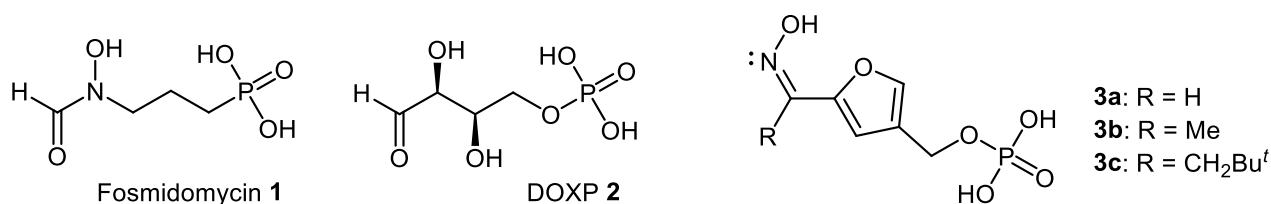


Figure 1. Structures of fosmidomycin **1**, DOXP **2** and the targeted ligands **3**.

Results and Discussion

Earlier *in silico* modelling,²² under rigid conditions using Autodock 4.0,²³ indicated the capacity of the furan derivative **3a** to adopt a stable conformation similar to fosmidomycin **1** in the active-site of a, then available, X-ray structure of *EcDXR* (2EGH).²⁴ Figure 2 illustrates the potential of the furan and Z-oxime oxygen atoms to coordinate the divalent Mg²⁺ cation *via* a six-membered chelate. (With the *E*-oxime a five-membered metal chelate may be envisaged involving the furan oxygen and oxime nitrogen atoms.) While the dihydro- and tetrahydrofuran analogues have exhibited similar alignment with DOXP **2**, our synthetic efforts have been focussed, initially, on the furan derivatives **3a-c**.

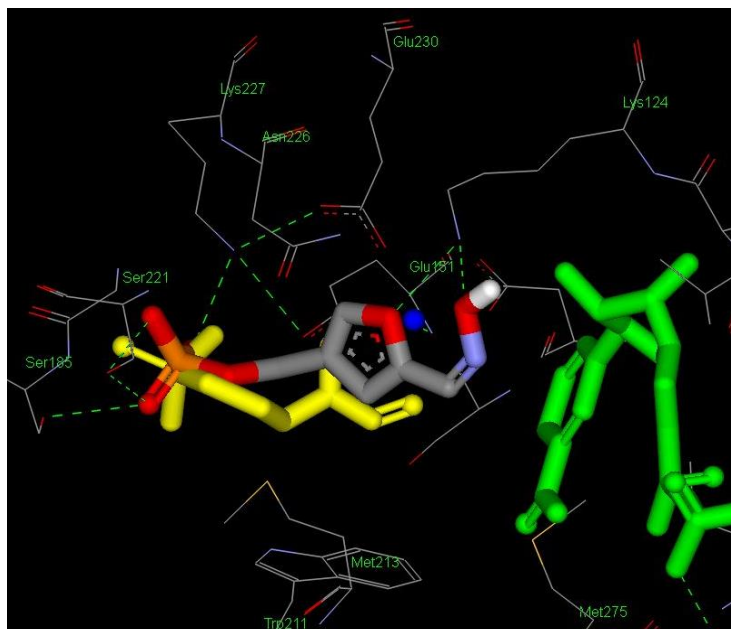
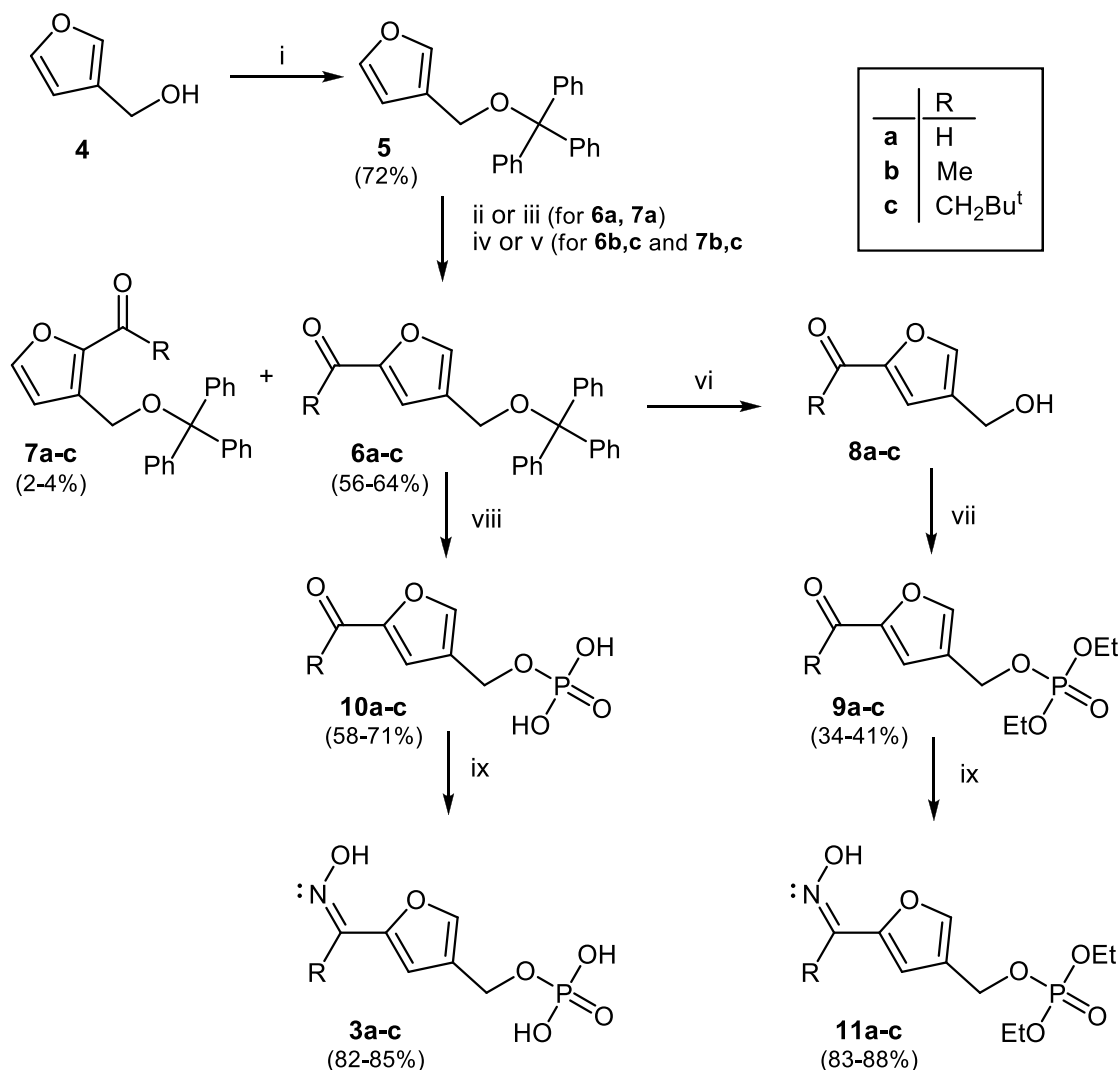


Figure 2. Initial rigid docking, using Autodock,²³ of ligand **3a** in the EcdXR active-site (2EGH),²⁴ illustrating hydrogen-bonding of the ligand with active-site residues. The crystal structure conformation of fosmidomycin **1** is coloured yellow, protein active-site residues are shown in wire-frame coloured by atom type, NADPH is coloured green, Mg²⁺ is shown as a blue sphere and the ligand **3a** is coloured by atom type. Hydrogen bonds are shown as green dashed lines.

Readily available 3-furanmethanol **4** appeared to be an appropriate substrate for the targeted 2,4-disubstituted furan derivatives **3a-c** and **11a-c** (Scheme 1). However, electrophilic substitution is favoured at both of the α -positions (C-2 and C-5) in furan^{25,26} and regioselective C-5 acylation of 3-furanmethanol **4** (C-2 in the product!) was clearly desirable. Moreover, since the initial approach was planned to involve a lithiation-acylation sequence, protection of the hydroxyl group in compound **4** was considered necessary. Tritylation was deemed a promising solution to both challenges since it would protect the hydroxyl group and the steric bulk of the resulting 3-(trityloxymethyl) group was expected to hinder competitive acylation at C-2 thus directing substitution to C-5. Reaction of 3-furanmethanol **4** with trityl chloride in the presence of excess triethylamine and a catalytic quantity of 4-dimethylaminopyridine (DMAP) afforded the protected intermediate **5** in 72% yield (Scheme 1).

In addition to introducing formyl (as in fosmidomycin **1**) and acetyl groups (as in FR900098), introduction of the 3,3-dimethylbutanoyl group was planned in order to explore the capacity of unoccupied hydrophobic cavities in the DXR-active site to accommodate the bulky *tert*-butyl group. Several methods for acylating the furan moiety of the tritylated derivative **5** were explored. The first, which involved treatment of the tritylated derivative **5** with *n*-butyllithium followed by reaction with DMF, resulted in a mixture shown by NMR analysis to contain the isomeric aldehydes **6a** and **7a**. Semi-preparative HPLC afforded the desired regioisomer **6a** as the major product, but in only 12% yield. Vilsmeier-Haak formylation²⁷ of the tritylated derivative **5** using phosphoryl chloride and DMF, however, furnished the desired aldehyde **6a** as the major product in 64% yield. The 5(formerly 2)-H signal is clearly evident at 6.74 ppm in the ¹H NMR spectrum of compound **6a** but is absent in the spectrum of the regioisomer **7a**, which was isolated in a yield of only 2.4%.

Friedel-Crafts methodology^{28,29} was employed to access the 5-acetyl- and 5-(3,3-dimethylbutanoyl) analogues **6b** and **6c**, respectively. While aluminium trichloride is commonly used as the Lewis acid catalyst in such reactions, it has been reported to induce polymerisation of furan derivatives³⁰ and attention was consequently given to the use of tin tetrachloride (SnCl₄) and zinc chloride (ZnCl₂) as alternative catalysts.^{31,32} Thus, the tritylated furan derivative **5** was reacted with acetic anhydride³³ and with 3,3-dimethylbutanoyl chloride using SnCl₄ and ZnCl₂ to afford the required acylated derivatives **6b** and **6c** as the major products; the regio-directing effect of the 3-(trityloxymethyl) group was certainly evident with the unwanted 2-substituted regioisomers being limited to trace quantities (< 3%). The reactions were conducted initially at 0 °C and then 40 °C, thus avoiding electrophilic substitution of the phenyl rings, marginally better yields being obtained for **6b** and **6c**, respectively with SnCl₄ (64 and 56%) than with ZnCl₂ (37 and 33%).



Scheme 1

Reagents and reaction conditions: i) Ph₃CCl, Et₃N, DMAP, THF, 80 °C, 15 h, N₂; ii) *n*-BuLi, THF, -30 °C, 4 h, N₂ then DMF, -30 °C, 2 h, r.t., 2 h.; iii) POCl₃, DMF, 0 °C for 2 h, 65 °C for 1 h then H₂O/NaOH; iv) Ac₂O or 3,3-dimethylbutanoyl chloride, SnCl₄, 0 °C for 1 h, 40 °C for 4 h, N₂; v) Ac₂O or 3,3-dimethylbutanoyl chloride, ZnCl₂, 0 °C for 1 h, 40 °C for 8 h, N₂; vi) HCOOH/THF/H₂O [1:1:0.1 v/v], 50 °C, 2 h; vii) diethyl chlorophosphate, pyridine, 0 °C, 1 h, r.t., overnight; viii) H₃PO₄/THF (1:1 v/v), r.t., 2 d; ix) NH₂OH.HCl, NaOAc, EtOH, reflux, 1 h.

While various methods have been reported for removing the trityl protecting group,³⁴⁻³⁶ we elected to use mild acid hydrolytic conditions,³⁷ involving treatment of compounds **6a-c** with formic acid in aqueous methanol for two hours at 50 °C. The resulting primary alcohols **8a-c** were used without further purification; reaction with diethyl chlorophosphate in pyridine gave the corresponding phosphate esters **9a-c** in 71-74% yield. The dihydrogen phosphate analogues **10a-c**, on the other hand, were accessed in moderate yields (58-65%) by subjecting compounds **6a-c** to tandem de-tritylation and phosphorylation using a mixture of H₃PO₄ and THF (1:1 v/v). The presence of the phosphate moiety in compounds (**9**) and (**10**) is confirmed by the splitting of ¹H and ¹³C NMR signals from ³¹P coupling with other proximate nuclei.

The final phase in our approach to the desired DOXP analogues involved oximation of the carbonyl compounds (**9**) and (**10**). While various oximation methodologies have been developed,³⁸⁻⁴⁰ we followed the classical method,⁴¹ which involved treating compounds **9a-c** and **10a-c** with an ethanolic solution of hydroxylamine hydrochloride in the presence of a catalytic quantity of sodium acetate. The corresponding, novel oximes **11a-c** and **3a-c** were isolated in good yields (87-96%) and were fully characterised. The phosphate esters **11a-c** might be expected to act as pro-drugs with better membrane permeability than their dihydrogen phosphate analogues **3a-c**, to which they could be hydrolysed *in vivo* by esterases.

Extensive *in silico* docking studies of compounds **3a-c** and **10a-c** [including all possible (de)protonation states and *E/Z* oxime geometries], and the phosphate esters **11a-c** and **9a-c** in *EcDXR* and/or *PfDXR* active sites have been undertaken. Autodock 4.2²³ docking in the initially available *EcDXR* X-ray structure (2EGH²⁴) had revealed that the most favourable conformation adopted by the formyl derivative **3a** within the active-site exhibited hydrogen-bonding interactions with the *rigidly held* proximal amino acid residues, Lys 124, Glu151, Ser185, Ser221, Lys227 and Glu230. Compound **3a** and its acetyl derivative **3b** exhibited comparable, respective binding affinities (-10.84 and -10.20 Kcal.mol⁻¹) and ligand efficiencies (-0.77 and -0.68). The furan ring not only restricts conformational flexibility between the phosphate- and metal-binding sites, but the endocyclic oxygen appears to exhibit a hydrogen-bonding interaction with Lys 124. The 3,3-dimethylbutanoyl analogue **3c**, however, appeared to be too bulky to be accommodated within the active-site, with the *tert*-butyl group extending well beyond the metal-binding site and resulting in a *ca.* 50% reduction in binding affinity (-5.89 Kcal.mol⁻¹) and ligand efficiency (-0.31).

In more detailed studies of the effect of steric bulk in determining the access and binding of ligands to *EcDXR* and *PfDXR* active sites, Autodock 4.2²³ and Autodock Vina⁴² were both used and the proximal receptor residues were set to be *flexible*. In addition, various protonation and stereochemical (*E*- and *Z*-oxime) options were considered for each of the compounds **3a-3c**. Each of the resulting ligand structures was docked against a range of *PfDXR* (homology-modelled,⁴³ 3AUA⁴⁴ and 3AU9⁴⁴) and *EcDXR* (2EGH²⁴ and 1Q0L⁴⁵) receptors. In all cases, binding of the potential *pro-drugs* **11a-c** was, unsurprisingly, less favourable than for the potential DXR inhibitors **3a-c**. Interestingly, in terms of binding energy, ligand binding to the *EcDXR* structures was favoured over the *PfDXR* structures. With Autodock 4.2²³ docking, the ligand poses proved highly sensitive to the protonation state and the *E/Z* geometry of the oxime moiety. Moreover, as evidenced by the relative binding energies (illustrated graphically in the Supplementary Information file), there was little consistency in ligand poses through the series. However, the binding energy data indicates that the **3a** (R = H) and **3b** (R = Me) species bind preferentially to the *PfDXR* structures, while the **3c** (R = CH₂Bu^t) species exhibits a preference for *EcDXR* (data tabulated and illustrated graphically in the Supplementary Information file). Given their structural similarity to DOXP, the 2-acylated furan derivatives **10a-c** and their diethyl ester analogues **9a-c** were also docked against the selected enzyme targets. In the light of these studies, some general observations can be made.

- i) Autodock Vina⁴² docking to a *rigid* receptor gave consistently weak binding energies indicative of poor binding for all the ligand systems examined. The QuickVina-W⁴⁶ and Autodock Vina⁴² results for binding to a *flexible* receptor generally reflect significantly stronger binding and the corresponding data sets are consistent with each other.
- ii) It is apparent that while **3a** and **3b** bind well to both *PfDXR* and *EcDXR* receptors, **3c** having the greatest steric bulk binds better to *EcDXR* (and to the *PfDXR* homology model⁴³ which is based on an *EcDXR* template).
- iii) Interestingly, **3a** and **3b** exhibit “reverse” binding in the active site of the *PfDXR* structure 3AU9_A,⁴⁴ in the sense that, in each of the ligands, the phosphate moiety, rather than the oxime moiety, is located close to the magnesium cation (Figure 3). In contrast, **3c** binds outside of the active site with weak binding affinity (-5.0 Kcal/mol). Other docking poses show **3c** penetrating a cleft in the protein to allow the phosphate moiety to coordinate to the Mg²⁺ cation, albeit with even weaker binding affinity (-4.6 Kcal/mol). Ligands **3a** and **3b**, on the other hand, exhibit good binding energies (-8.1 and -8.5 Kcal.mol⁻¹, respectively). These binding energies should be seen in the context of the corresponding values for the known inhibitors, FR900098 and fosmidomycin **1**, to 3AU9_A⁴⁴ (-8.2 Kcal.mol⁻¹ in both instances).
- iv) Similar orientation patterns emerge (Figure 4) for binding to the *EcDXR* receptor 2EGH_B²⁴ with **3a** and **3b** almost perfectly overlaid in a “reverse” orientation. However **3c** now binds in the “normal” orientation, in that the oxime moiety binds close to the Mg²⁺ cation. It is also apparent, however, that all three of the ligands **3a-c** bind orthogonally to the co-crystallized ligand, fosmidomycin **1**, but ligand **3c** exhibits the strongest binding affinity for this receptor (-9.6s Kcal.mol⁻¹ compared to -8.0 and -8.4 Kcal.mol⁻¹ for **3a** and **3b**, respectively). Again, this is in the context of the binding of FR900098 and fosmidomycin **1** to 2EGH_B²⁴ (-8.2 and -7.3 Kcal.mol⁻¹, respectively).
- v) Weak docking scores were observed for the phosphate esters **9a-c** across all targets. While the structural variants for **10c** exhibit good binding to the *EcDXR* targets (and the *PfDXR* homology model⁴³), they bind poorly to the *PfDXR* targets (*e.g.*, -7.3 Kcal.mol⁻¹ to *PfDXR* 3AU9_B⁴⁴). The 2-formyl and 2-acetyl DOXP analogues **10a** and **10b**, however, exhibit good binding scores across all targets – particularly to *PfDXR* targets. In fact, their binding affinities for *PfDXR* 3AU9_B⁴⁴ (**10a**, -8.1; **10b**, -8.4) are comparable with that of the natural enzyme substrate, DOXP (-8.5 Kcal.mol⁻¹). Moreover, in terms of pose, the docking of DOXP and **10a-b** to 3AU9_B,⁴⁴ for example, clearly matches the fosmidomycin **1** pose in the crystal structure, as illustrated in Figure 5. Ligand **10c**, however, is too large to be accommodated within the active site, and its best pose penetrates through the enzyme structure to coordinate the Mg²⁺ cation.

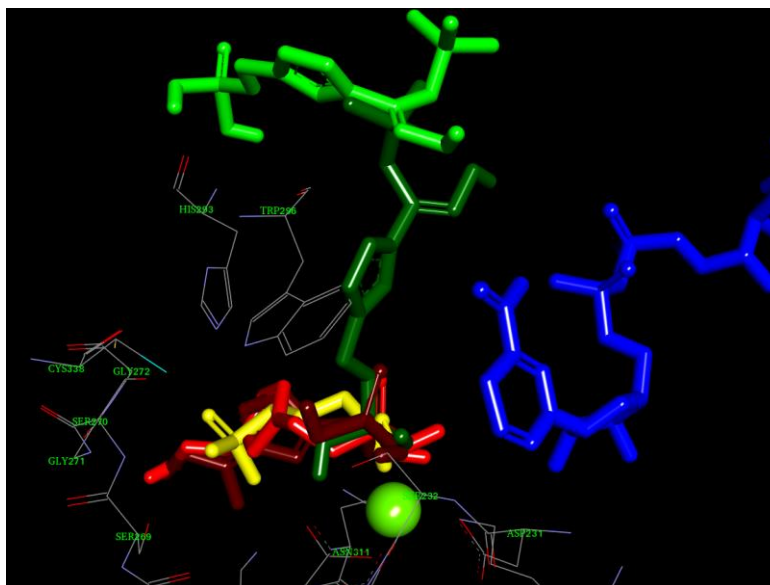


Figure 3. Best binding poses of **3a** (red) and **3b** (brown) to the *PfDXR* structure 3AU9_A⁴⁴ showing reverse binding (with phosphate close to the Mg²⁺ cation) relative to fosmidomycin **1** yellow. **3c** binds externally (light green) with higher energy poses penetrating the active site (dark green). The cofactor is shown in blue and the Mg cation as a sphere.

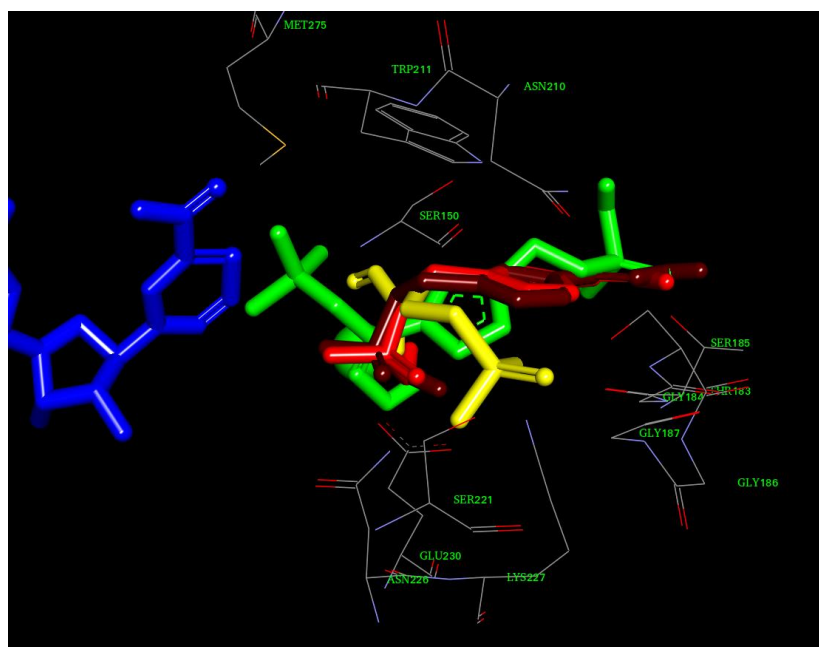


Figure 4. Best binding poses of **3a** (red) and **3b** (brown) to the *EcDXR* structure 2EGH_B²⁴ showing “reverse” binding (with phosphate close to the Mg²⁺ cation). **3c** (green) interacts with the Mg (behind) in a similar manner to fosmidomycin **1** (yellow). The cofactor is shown in blue and the Mg²⁺ cation (behind) as a green sphere.

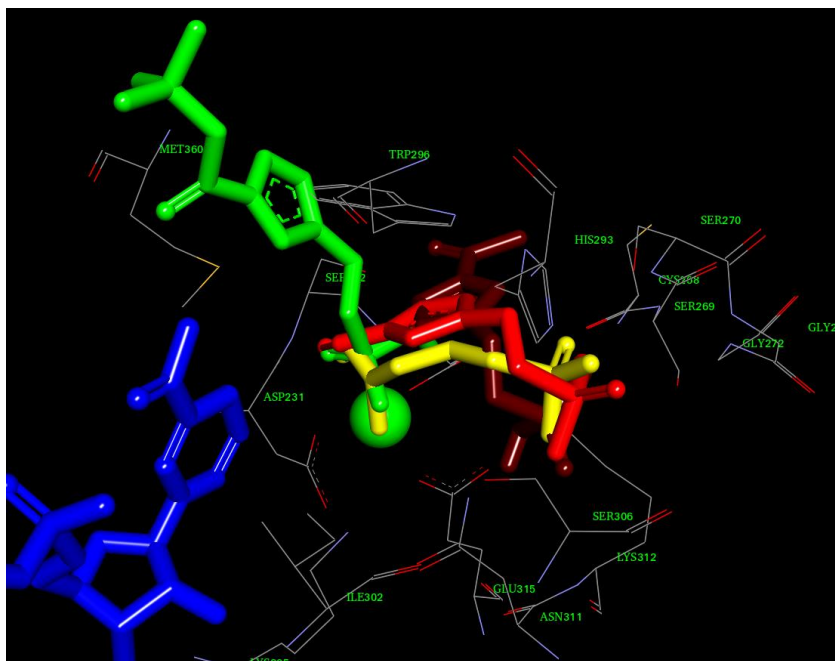


Figure 5. Best binding poses of **10a** (red), **10b** (brown) and **10c** (green) to the *PfDXR* structure 3AU9_B.⁴⁴ **10a** and **10b**, together with **DOXP** (not shown) bind in an arrangement similar to fosmidomycin **1** (yellow). **10c** penetrates through to the active site. The cofactor is shown in blue and the Mg^{2+} cation as a sphere.

Conclusions

A series of novel (2-substituted furan-4-yl)methyl dihydrogen phosphates (**3a-c**) and (**10a-c**) and their corresponding diethyl derivatives (**11a-c**) and (**9a-c**) have been prepared regioselectively. The formyl and acetyl derivatives **3a** and **3b** had earlier been subjected²² to Saturation Transfer Difference (STD) NMR binding studies using the then available *EcDXR* enzyme; both compounds gave positive STD results (illustrated in the Supporting Information file). While the STD NMR data does not preclude the possibility of allosteric or non-competitive binding, these results are clearly consistent with the significant *in silico* binding data of the oximes **3a** and **3b** and the DOXP analogues **10a** and **10b** in *PfDXR* enzyme active sites. These results, coupled with the possibility of the corresponding diethyl phosphate esters (**9**) and (**11**) serving as potential pro-drugs, will encourage future research on the synthesis of dihydro- and tetrahydrofuran analogues and the capacity of such conformationally constrained ligands to inhibit the action of the *PfDXR* enzyme and, hence, the growth of the *P. falciparum* parasite. The *PfDXR* enzyme is now readily over-expressed and purified using heterologous expression systems,⁴⁷ enabling the future screening of these furan derivatives for novel inhibitors of this anti-malarial drug target.

Experimental Section

General. NMR spectra were recorded on Bruker AVANCE 400 or BIOSPIN 600 MHz spectrometers in $CDCl_3$, $DMSO-d_6$ or CD_3OD , and were calibrated using solvent signals. Melting points were measured using a hot-stage apparatus and are uncorrected. High-resolution mass spectra (HRMS) were recorded on a Waters API Q-TOF

Ultima spectrometer (University of Stellenbosch, Stellenbosch, South Africa) and elemental analyses were obtained on a Vario Elemental Microtube EL III analyser. STD NMR and computer modelling protocols have been published previously.¹⁶ Representative NMR spectra are provided in the Supporting Information.

3-[(Trityloxy)methyl]furan (5). A solution of triphenylmethyl chloride (6.00 g, 21 mmol), 3-furanmethanol (**4**) (2.00 g, 20.4 mmol), triethylamine (4.5 mL, 3.24g, 32 mmol) and DMAP (0.61 g, 5.0 mmol) in THF (30 mL) was stirred under N₂ at 80 °C for 15 hours. The solvent was evaporated *in vacuo* and the residue dissolved in EtOAc (100 mL). The organic phase was washed sequentially with water (2 x 50 mL) and brine (2 x 50 mL). The aqueous washings were extracted with EtOAc and the organic layers were combined and dried (anhydr. MgSO₄). The solvent was evaporated *in vacuo* to afford 3-[(trityloxy)methyl]furan **5** as a yellow gum (4.98 g, 72%) [δ_{H} /ppm (400 MHz; CDCl₃) 4.06 (2H, s, OCH₂), 6.43 (1H, s, 2-H), 7.27 – 7.54 (17H, m, 4-H, 5-H and trityl group); δ_{C} /ppm (100 MHz; CDCl₃) 58.4 (OCH₂), 86.9 (C-2'), 109.9 (C-4), 123.1 (C-3), 127.0 (C-6'), 127.8 (C-4' and C-8'), 128.6 (C-5' and C-7'), 139.7 (C-3'), 143.0 (C-2) and 144.0 (C-5)], which was used without further purification.

The two procedures for the synthesis and characterisation of compounds 6a and 7a are illustrated below.

Method 1. To a stirred solution of 3-[(trityloxy)methyl]furan **5** (2.00 g, 5.88 mmol) in THF (20 mL) under N₂ at ca. -30 °C, *n*-butyllithium (ca. 1.5 M in hexane; 6.0 mL, 9 mmol) was slowly added dropwise *via* a septum, ensuring that the temperature did not exceed -30 °C. The resulting mixture was stirred for 4 hours; DMF (1.38 mL) was then added and the mixture stirred for a further 2 hours. The reaction mixture was allowed to warm to room temperature and stirred for an additional 2 hours before being quenched with water (15 mL) and extracted with diethyl ether (2 x 50 mL). The organic extracts were washed sequentially with 10% aq. NaHCO₃ (2 x 50 mL), brine (2 x 50 mL) and dried (anhydr. MgSO₄). The solvent was removed *in vacuo* to obtain the crude product as a yellow solid. A portion of the crude product was purified [normal-phase HPLC; elution with hexane-EtOAc (4:1)] to yield two products.

(i) 4-[(Trityloxy)methyl]furan-2-carbaldehyde (6a) as a pale yellow solid (12%); δ_{H} /ppm (400 MHz; CDCl₃) 4.45 (2H, s, OCH₂), 6.75 (1H, s, 5-H), 7.26 – 7.49 (15H, m, trityl group), 7.61 (1H, s, 3-H) and 9.73 (1H, s, CHO); δ_{C} /ppm (100 MHz; CDCl₃) 57.8 (OCH₂), 87.3 (C-2'), 120.5 (C-3), 126.4 (C-4), 127.2 (C-6') 128 (C-4' and C-8'), 128.5 (C-5' and C-7'), 143.6 (C-3'), 145.2 (C-5), 153.1 (C-2) and 178.0 (C=O); and

(ii) the regioisomer, 3-[(Trityloxy)methyl]furan-2-carbaldehyde (7a) as a white solid (4%); δ_{H} /ppm (400 MHz; CDCl₃) 4.14 (2H, s, OCH₂), 7.31 – 7.69 (17H, m, 4-H, 5-H and trityl group) and 9.68 (1H, s, CHO); δ_{C} /ppm (100 MHz; CDCl₃) 58.1 (OCH₂), 87.6 (C-2'), 113.1 (C-4), 127.3 (C-6'), 128.0 (C-4' and C-8'), 128.6 (C-5' and C-7'), 135.4 (C-3), 143.5 (C-3'), 147.2 (C-5), 147.8 (C-2) and 178.5 (C=O).

Method 2. The Vilsmeier reagent was prepared by adding phosphorus oxychloride (1.86 mL, 3.05g, 20.0 mmol) dropwise to DMF (20 mL) under nitrogen over a period of 30 min, maintaining the temperature below 5 °C. The mixture was stirred for 30 min, after which 3-[(trityloxy)methyl]furan **5** (2.00 g, 5.88 mmol) in DMF (5 mL) was added. The reaction mixture was stirred for 3 hours at room temperature and then heated at 80 °C for 1 hour. After cooling, the mixture was poured into ice-water (200 mL) and the pH adjusted to pH 10 with 0.1 M aq. NaOH. The solution was extracted with diethyl ether (4 x 50 mL), and the organic extracts were combined, washed with water and brine and the dried (anhydr. MgSO₄). The solvent was removed *in vacuo* to afford the crude product, which was recrystallised from MeOH to yield 4-[(trityloxy)methyl]furan-2-carbaldehyde **6a** as pale-yellow crystals (1.39 g, 64%).

The general procedure for the synthesis and characterisation of compounds 6b and 6c is illustrated by the following example. Acetic anhydride (0.27 mL, 2.9 mmol) was added dropwise to a solution of SnCl₄ (0.12 mL, 0.27g, 1.0 mmol) in DCM (10 mL) under N₂ at 0 °C and the mixture was stirred for 15 min. 3-

[(Trityloxy)methyl]furan (**5**) (1.00 g, 2.94 mmol) in DCM (10 mL) was added and the reaction mixture was stirred at 0 °C for 1 hour. The reaction mixture was then warmed to 40 °C and stirred for 4 hours. After completion, the mixture was treated with saturated aq. NaHCO₃ (50 mL) and extracted with diethyl ether (2 x 50 mL). The organic extracts were combined, dried (anhydr. MgSO₄) and filtered. The solvent was removed under reduced pressure and a portion of the residue was purified [normal-phase HPLC; elution with hexane-EtOAc (3:1)] to yield two products.

(i) 2-Acetyl-4-[(trityloxy)methyl]furan (6b). Yellow oil (64%); ν/cm^{-1} 1675 (C=O); $\delta_{\text{H}}/\text{ppm}$ (400 MHz; CDCl₃) 2.57 (3H, s, CH₃CO), 4.42 (2H, s, OCH₂) and 7.14 - 7.34 (17H, m, 3-H, 5-H and trityl group); $\delta_{\text{C}}/\text{ppm}$ (100 MHz; CDCl₃) 24.2 (CH₃), 57.3 (OCH₂), 87.6 (C-2'), 120.4 (C-3), 126.4 (C-4), 127.4 (C-6') 127.9 (C-4' and C-8'), 128.4 (C-5' and C-7'), 143.5 (C-3'), 145.3 (C-5), 153.5 (C-2) and 181.3 (C=O); (Found: C, 81.58; H, 5.76%. C₂₆H₂₂O₃ requires C, 81.65; H, 5.80%); and

(ii) the regioisomer, 2-Acetyl-3-[(trityloxy)methyl]furan (7b). Yellow oil (2%); ν/cm^{-1} 1682 (C=O); $\delta_{\text{H}}/\text{ppm}$ (400 MHz; CDCl₃) 2.59 (3H, s, CH₃CO), 4.45 (2H, s, OCH₂) and 7.12 - 7.28 (17H, m, 4-H, 5-H and trityl group); $\delta_{\text{C}}/\text{ppm}$ (100 MHz; CDCl₃) 24.8 (CH₃), 56.8 (OCH₂), 87.3 (C-2'), 112.8 (C-4), 126.7 (C-6'), 128.1 (C-4' and C-8'), 128.8 (C-5' and C-7'), 134.6 (C-3), 143.6 (C-3'), 147.3 (C-2), 148.2 (C-5) and 181.8 (C=O) (Found: C, 81.60; H, 5.82%. C₂₆H₂₂O₃ requires C, 81.65; H, 5.80%).

2-(3,3-Dimethylbutanoyl)-4-[(trityloxy)methyl]furan (6c). Yellow oil (56%); ν/cm^{-1} 1685 (C=O); $\delta_{\text{H}}/\text{ppm}$ (400 MHz; CDCl₃) 1.19 (9H, s, 3 x CH₃), 2.58 (2H, s, CH₂CO), 4.47 (2H, s, OCH₂) and 7.19 - 7.31 (17H, m, 3-H, 5-H and trityl group); $\delta_{\text{C}}/\text{ppm}$ (100 MHz; CDCl₃) 29.1 (3 x CH₃), 30.2 (C-3''), 47.4 (C-2''), 57.9 (OCH₂), 87.4 (C-2'), 120.6 (C-3), 126.4 (C-4), 127.3 (C-6') 128.0 (C-4' and C-8'), 128.6 (C-5' and C-7'), 143.7 (C-3'), 145.3 (C-5), 153.2 (C-2) and 187.0 (C=O); (Found: C, 82.30; H, 6.78%. C₃₀H₃₀O₃ requires C, 82.16; H, 6.89%).

2-(3,3-Dimethylbutanoyl)-3-[(trityloxy)methyl]furan (7c). Yellow oil (3%); (Found: C, 82.35; H, 6.83%. C₃₀H₃₀O₃ requires C, 82.16; H, 6.89%); ν/cm^{-1} 1691 (C=O); $\delta_{\text{H}}/\text{ppm}$ (400 MHz; CDCl₃) 1.21 (9H, s, 3 x CH₃), 2.56 (2H, s, CH₂CO), 4.52 (2H, s, OCH₂) and 7.14 - 7.21 (17H, m, 4-H, 5-H and trityl group); $\delta_{\text{C}}/\text{ppm}$ (100 MHz; CDCl₃) 29.5 (3 x CH₃), 31.3 (C-3''), 46.8 (C-2''), 58.2 (OCH₂), 87.3 (C-2'), 113.2 (C-4), 126.6 (C-6'), 127.8 (C-4' and C-8'), 128.9 (C-5' and C-7'), 132.8 (C-3), 143.8 (C-3'), 145.7 (C-5), 146.4 (C-2) and 186.4 (C=O); (Found: C, 82.35; H, 6.83%. C₃₀H₃₀O₃ requires C, 82.16; H, 6.89%).

General procedure for the synthesis of compounds 8a-c, which were used without further purification, is illustrated by the following example. (Compounds **8a,b** are known.⁴⁸) A suspension of 2-(3,3-dimethylbutanoyl)-4-[(trityloxy)methyl]furan (**6c**) (0.25 g, 0.57 mmol) in HCOOH-THF-H₂O (1:1:0.1; 5 mL) was heated at 50 °C for 2 hours. The solvent was removed *in vacuo*, [co-evaporated with hexane (2 x 10 mL)] to yield 2-(3,3-dimethylbutanoyl)-4-(hydroxymethyl)furan (**8c**) as a colourless oil [$\delta_{\text{H}}/\text{ppm}$ (400 MHz; CDCl₃) 1.19 (9H, s, 3 x CH₃), 2.12 (1H, s, OH), 2.54 (2H, s, CH₂CO), 4.52 (2H, s, OCH₂), 6.41 (1H, s, 5-H) and 7.39 (1H, s, 3-H); $\delta_{\text{C}}/\text{ppm}$ (100 MHz; CDCl₃) 28.6 (3 x CH₃), 32.6 (C-3'), 36.7 (C-2'), 58.6 (CH₂OH), 120.2 (C-3), 123.8 (C-4), 145.3 (C-5), 153.2 (C-2) and 184.7 (C=O)] which was used without further purification.

General procedure for the synthesis of compounds 9a-c is illustrated by the following example. Diethyl chlorophosphate (0.52 g, 3.0 mmol) was added slowly to a stirred solution of 4-(hydroxymethyl)furan-2-carbaldehyde (**8a**) (0.20 g, 1.6 mmol) in pyridine (10 mL) at 0 °C. The reaction mixture was allowed to reach room temperature and then stirred for 24 hours. The solvent was removed *in vacuo* and the residue was dissolved in DCM (25 mL). The organic phase was washed with satd. aq. NaHCO₃ (2 x 50 mL), water (2 x 50 mL) and brine (2 x 50 mL), and dried (anhydr. MgSO₄). The solvent was evaporated *in vacuo* and the residue chromatographed [preparative layer chromatography; elution with hexane-EtOAc (4:1)] to yield **diethyl (2-formylfuran-4-yl)methyl phosphate (9a)** as a clear oil (0.14 g, 34%); ν/cm^{-1} 1677 (C=O) and 1227 (P=O); $\delta_{\text{H}}/\text{ppm}$ (400 MHz; CDCl₃) 1.29 (6H, m, 2 x CH₃), 4.10 (4H, m, 2 x CH₂CH₃), 4.87 (2H, d, *J* 2.2 Hz, OCH₂), 6.45 (1H,

s, 5-H), 7.39 (1H, s, 3-H) and 10.12 (1H, s, CHO); δ_C /ppm (100 MHz; CDCl₃) 16.3 (d, J_{F-C} 6.1 Hz, 2 x CH₃), 60.8 (d, J_{P-C} 6.4 Hz, OCH₂), 61.4 (d, J_{P-C} 6.6 Hz, 2 x CH₂CH₃), 120.3 (C-3), 125.6 (C-4), 145.3 (C-5), 153.2 (C-2) and 181.7 (C=O); (Found: C, 45.90; H, 5.84%. C₁₀H₁₅O₆P requires C, 45.81; H, 5.77%).

(2-Acetylfuran-4-yl)methyl diethyl phosphate (9b). Yellow oil (0.15 g, 38%); ν /cm⁻¹ 1680 (C=O) and 1223 (P=O); δ_H /ppm (400 MHz; CDCl₃) 1.30 (6H, t, J 6.8 Hz, 2 x CH₂CH₃), 2.54 (3H, s, CH₃CO), 4.07 (4H, m, 2 x CH₂CH₃), 5.05 (2H, d, J 1.6 Hz, OCH₂), 7.11 (1H, s, 5-H) and 7.13 (2H, s, 3-H); δ_C /ppm (100 MHz; CDCl₃) 16.3 (d, J_{P-C} 6.0 Hz, 2 x CH₃), 24.6 (CH₃CO), 61.5 (d, J_{P-C} 6.5 Hz, OCH₂ and 2 x CH₂CH₃), 120.8 (C-3), 122.9 (C-4), 145.7 (C-5), 150.1 (C-2) and 182.6 (C=O); (Found: C, 48.01; H, 6.15%. C₁₁H₁₇O₆P requires C, 47.83; H, 6.20%).

Diethyl [2-(3,3-dimethylbutanoyl)furan-4-yl]methyl phosphate (9c). Yellow oil (0.14 g, 41%); ν /cm⁻¹ 1681 (C=O) and 1232 (P=O); δ_H /ppm (400 MHz; CDCl₃) 1.21 (9H, s, 3 x CH₃), 1.31 (6H, t, J 6.8 Hz, 2 x CH₂CH₃), 2.56 (2H, s, CH₂CO), 4.08 (4H, m, 2 x CH₂CH₃), 5.09 (2H, d, J 1.6 Hz, OCH₂), 6.47 (1H, s, 5-H) and 7.12 (1H, s, 3-H); δ_C /ppm (100 MHz; CDCl₃) 16.3 (d, J_{P-C} 6.1 Hz, 2 x CH₂CH₃), 29.2 (3 x CH₃), 32.3 (C-3'), 36.8 (C-2'), 62.3 (d, J_{P-C} 6.5 Hz, OCH₂ and 2 x CH₂CH₃), 120.5 (C-3), 124.2 (C-4), 145.7 (C-5), 153.4 (C-2) and 185.3 (C=O); (Found: C, 54.30; H, 7.60%. C₁₅H₂₅O₆P requires C, 54.21; H, 7.58%).

General procedure for the synthesis of compounds 10a-c is illustrated by the following example. A solution of 4-[(trityloxy)methyl]furan-2-carbaldehyde (**6a**) (0.30 g, 0.82 mmol) and H₃PO₄/THF (1:1 v/v; 2.0 mL) was stirred at room temperature for ca. 2 days. The solvent was removed under reduced pressure and the residue dissolved in EtOAc (25 mL). The organic phase was washed with 10% aq. NaHCO₃ (2 x 50 mL), and the aqueous layers were collected and acidified (pH 2.0) with 0.1M-HCl. The aqueous phase was extracted with EtOAc (3 x 25 mL) and the combined organic solutions were dried (anhydr. MgSO₄). The solvent was evaporated *in vacuo* and the residue chromatographed [preparative layer chromatography; elution with hexane-EtOAc-MeOH (1:1:1)] to yield **(2-formylfuran-4-yl)methyl dihydrogen phosphate (10a)**. Yellow oil (71%); ν /cm⁻¹ 1673 (C=O) and 1234 (P=O); δ_H /ppm (400 MHz; D₂O) 5.11 (2H, d, J 1.6 Hz, OCH₂), 7.10 (1H, s, 5-H), 7.40 (1H, s, 3-H) and 9.74 (1H, s, CHO); δ_C /ppm (100 MHz; D₂O) 61.9 (d, J_{P-C} 6.4 Hz, 2 x OCH₂), 120.9 (C-3), 123.0 (C-4), 145.8 (C-5), 150.2 (C-2) and 180.0 (C=O); (Found: C, 35.01; H, 3.49%. C₆H₇O₆P requires C, 34.97; H, 3.42%).

(2-Acetylfuran-4-yl)methyl dihydrogen phosphate (10b). Colourless oil (61%); ν /cm⁻¹ 1687 (C=O) and 1241 (P=O); δ_H /ppm (400 MHz; D₂O) 2.61 (3H, s, CH₃CO), 5.07 (2H, d, J 2.3 Hz, OCH₂), 7.12 (1H, s, 5-H) and 7.35 (1H, s, 3-H); δ_C /ppm (100 MHz; D₂O) 24.3 (CH₃), 62.3 (d, J_{P-C} 6.5 Hz, OCH₂), 120.7 (C-3), 122.9 (C-4), 145.5 (C-5), 153.2 (C-2) and 182.3 (C=O); (Found: C, 38.27; H, 4.09%. C₇H₉O₆P requires C, 38.20; H, 4.12%).

[2-(3,3-Dimethylbutanoyl)furan-4-yl]methyl dihydrogen phosphate (10c). Colourless oil (58%); (Found: C, 47.91; H, 6.11%. C₁₁H₁₇O₆P requires C, 47.83; H, 6.20%); ν /cm⁻¹ 3307 (OH), 1687 (C=O) and 1231 (P=O); δ_H /ppm (400 MHz; D₂O) 1.21 (9H, s, 3 x CH₃), 2.55 (2H, s, CH₂CO), 5.02 (2H, d, J 2.4 Hz, OCH₂), 7.15 (1H, s, 5-H) and 7.39 (1H, s, 3-H); δ_C /ppm (100 MHz; D₂O) 29.3 (3 x CH₃), 32.2 (C-3'), 36.8 (C-2'), 62.2 (d, J_{P-C} 6.5 Hz, OCH₂), 120.4 (C-3), 123.7 (C-4), 145.5 (C-5), 152.8 (C-2) and 185.6 (C=O). (Found: C, 47.91; H, 6.11%. C₁₁H₁₇O₆P requires C, 47.83; H, 6.20%).

General procedure for the synthesis of compounds 11a-c is illustrated by the following example. Diethyl (2-formylfuran-4-yl)methyl phosphate (**9a**) (0.11 g, 0.42 mmol), hydroxylamine hydrochloride (0.10 g, 1.4 mmol) and sodium acetate (0.020 g, 0.24 mmol) were dissolved in EtOH (8 mL) and the mixture was refluxed for 1 hour. After completion of the reaction, the solvent was removed under reduced pressure and the residue was dissolved in diethyl ether (20 mL). The organic layer was washed sequentially with water (20 mL) and brine (20 mL), and dried (anhydr. Na₂SO₄). The solvent was removed *in vacuo* and the residue chromatographed [preparative layer chromatography; elution with hexane-EtOAc (4:1)] to yield **diethyl {2-[(N-hydroxyimino)methyl]furan-4-yl}methyl phosphate (11a)**. Colourless oil (97 mg, 83%); (Found: C, 43.47; H, 5.69; N, 5.11%. C₁₀H₁₆NO₆P requires C, 43.33; H, 5.82; N, 5.05%); ν /cm⁻¹ 3271 (OH), 1651 (C=N) and 1218

(P=O); δ_{H} /ppm (400 MHz; CDCl_3) 1.28 (6H, m, 2 x CH_3), 4.08 (4H, m, 2 x CH_2CH_3), 5.05 (2H, d, J 2.0 Hz, OCH_2), 6.44 (1H, s, 5-H), 7.41 (1H, s, 3-H), 8.17 (1H, s, OH) and 9.89 (1H, s, aldehydic proton); δ_{C} /ppm (100 MHz; CDCl_3) 16.2 (d, $J_{\text{P-C}}$ 6.5 Hz, 2 x CH_3), 59.8 (d, $J_{\text{P-C}}$ 6.4 Hz, OCH_2), 61.3 (d, $J_{\text{F-C}}$ 6.5 Hz, 2 x CH_2CH_3), 110.7 (C-3), 125.7 (C-4), 145.1 (C-5), 149.6 (C=N) and 153.7 (C-2).

Diethyl {2-[1-(*N*-hydroxyimino)ethyl]furan-4-yl}methyl phosphate (11b). Colourless oil (91 mg, 86%); ν/cm^{-1} 3243 (OH), 1672 (C=N) and 1225 (P=O); δ_{H} /ppm (400 MHz; CDCl_3) 1.31 (6H, t, J 7.2 Hz, 2 x CH_3), 2.53 (3H, s, $\text{CH}_3\text{C}=\text{N}$), 4.09 (4H, m, 2 x CH_2CH_3), 5.02 (2H, d, J 2.0 Hz, OCH_2), 5.87 (1H, s, OH), 6.48 (1H, s, 5-H) and 7.11 (1H, s, 3-H); δ_{C} /ppm (100 MHz; CDCl_3) 13.0 ($\text{CH}_3\text{C}=\text{N}$) 16.3 (d, $J_{\text{P-C}}$ 6.0 Hz, 2 x CH_3), 61.7 (d, $J_{\text{P-C}}$ 6.4 Hz, OCH_2 and 2 x CH_2CH_3), 109.8 (C-3), 127.2 (C-4), 143.7 (C-5), 148.5 (C=N) and 151.3 (C-2). (Found: C, 45.27; H, 6.14; N, 4.88%. $\text{C}_{11}\text{H}_{18}\text{NO}_6\text{P}$ requires C, 45.36; H, 6.23; N, 4.81%).

Diethyl {2-[1-(*N*-hydroxyimino)-3,3-dimethylbutyl]furan-4-yl}methyl phosphate (11c). Colourless oil (92 mg, 88%); ν/cm^{-1} 3281 (OH) 1663 (C=N) and 1218 (P=O); δ_{H} /ppm (400 MHz; CDCl_3) 1.15 (9H, s, 3 x CH_3), 1.26 (6H, t, J 6.8 Hz, 2 x CH_2CH_3), 2.55 (2H, $\text{CH}_2\text{C}=\text{N}$), 4.03 (4H, m, 2 x CH_2CH_3), 4.98 (2H, d, J 1.6 Hz, OCH_2), 5.67 (1H, s, OH), 6.50 (1H, s, 5-H) and 7.12 (1H, s, 3-H); δ_{C} /ppm (100 MHz; CDCl_3) 16.2 (d, $J_{\text{P-C}}$ 6.0 Hz, 2 x CH_2CH_3), 28.6 (3 x CH_3), 32.4 (C-3'), 36.6 (C-2'), 62.0 (OCH_2), 62.1 (d, $J_{\text{P-C}}$ 6.7 Hz, 2 x CH_2CH_3), 110.3 (C-3), 127.6 (C-4), 143.3 (C-5), 149.8 (C=N) and 153.4 (C-2). (Found: C, 51.79; H, 7.49; N, 3.97%. $\text{C}_{15}\text{H}_{26}\text{NO}_6\text{P}$ requires C, 51.87; H, 7.54; N, 4.03%).

General procedure for the synthesis of compounds 3a-c is illustrated by the following example. (2-Formylfuran-4-yl)methyl dihydrogen phosphate (**10a**) (0.10 g, 0.49 mmol), hydroxylamine hydrochloride (0.10 g, 1.4 mmol) and sodium acetate (0.020 g, 0.24 mmol) were dissolved in EtOH (8 mL) and the mixture was refluxed for 1 hour. After completion of the reaction, the solvent was removed under reduced pressure and the residue was dissolved in diethyl ether (20 mL). The organic solution was washed sequentially with water (20 mL) and brine (20 mL), and dried (anhydr. Na_2SO_4). The solvent was removed *in vacuo* and the residue chromatographed [preparative layer chromatography; elution with hexane-EtOAc-MeOH (1:1:1)] to yield **{2-[1-(*N*-hydroxyimino)methyl]furan-4-yl}methyl dihydrogen phosphate (3a)**. Colourless oil (88 mg, 82%); (Found: C, 32.71; H, 3.72; N, 6.30%. $\text{C}_6\text{H}_8\text{NO}_6\text{P}$ requires C, 32.59; H, 3.65; N, 6.33%); ν/cm^{-1} 3245 (OH), 1657 (CH=N) and 1232 (P=O); δ_{H} /ppm (400 MHz; $\text{DMSO}-d_6$) 3.57 (2H, s, 2 x OH), 5.11 (2H, d, J 2.0 Hz, OCH_2), 5.89 (1H, s, CH=N), 7.10 (1H, s, 5-H), 7.37 (1H, s, 3-H) and 9.41 (1H, s, NOH); δ_{C} /ppm (100 MHz; $\text{DMSO}-d_6$) 62.2 (d, $J_{\text{P-C}}$ = 5.9 Hz, OCH_2), 110.1 (C-3), 127.0 (C-4), 143.2 (C-5), 150.7 (C=NOH) and 151.8 (C-2).

{2-[1-(*N*-Hydroxyimino)ethyl]furan-4-yl}methyl dihydrogen phosphate (3b). Colourless oil (91 mg, 85%); ν/cm^{-1} 3253 (OH), 1648 (HC=N) and 1228 (P=O); δ_{H} /ppm (400 MHz; $\text{DMSO}-d_6$) 2.37 (3H, s, CH_3), 3.90 (2H, s, 2 x OH), 5.11 (2H, d, J 2.0 Hz, OCH_2), 7.12 (1H, s, 5-H), 7.32 (1H, s, 3-H) and 8.93 (1H, s, NOH); δ_{C} /ppm (100 MHz; $\text{DMSO}-d_6$) 13.2 (CH_3), 62.5 (d, $J_{\text{P-C}}$ = 6.3 Hz, OCH_2), 110.2 (C-3), 127.1 (C-4), 143.7 (C-5), 150.8 (C=NOH) and 153.3 (C-2); (Found: C, 35.84; H, 4.31; N, 5.32%. $\text{C}_7\text{H}_{10}\text{NO}_6\text{P}$ requires C, 35.76; H, 4.29; N, 5.29%).

{2-[1-(*N*-Hydroxyimino)-3,3-dimethylbutyl]furan-4-yl}methyl dihydrogen phosphate (3c). Colourless oil (87 mg, 83%); ν/cm^{-1} 3260 (OH), 1678 (HC=N) and 1229 (P=O); δ_{H} /ppm (400 MHz; $\text{DMSO}-d_6$) 1.12 (9H, s, 3 x CH_3), 1.83 (2H, s, $\text{CH}_2\text{C}=\text{N}$), 2.31 (2H, s, 2 x OH), 5.09 (2H, d, J 1.6 Hz, OCH_2), 7.17 (1H, s, 5-H), 7.32 (1H, s, 3-H) and 10.41 (1H, s, NOH); δ_{C} /ppm (100 MHz; $\text{DMSO}-d_6$) 29.0 (3 x CH_3), 32.6 (C-3'), 36.3 (C-2'), 62.3 (d, $J_{\text{P-C}}$ 6.6 Hz, OCH_2), 110.8 (C-3), 127.5 (C-4), 142.7 (C-5), 150.3 (C=NOH) and 152.2 (C-2); (Found: C, 45.29; H, 6.31; N, 4.79%. $\text{C}_{11}\text{H}_8\text{NO}_6\text{P}$ requires C, 45.36; H, 6.23; N, 4.81%).

Molecular Docking Protocols

The receptors used included *Ec*DXR 2EGH²⁴ (both chains A and B from the crystal structure) and 1Q0L, and *Pf*DXR structures 3AUA⁴⁴ and 3AU9⁴⁴ (both chains A and B) together with a homology model⁴³ (a *Pf*DXR structure created using an *Ec*DXR structure 1Q0Q⁴⁵ as one of three templates). The structures **3a-c** and **10a-c** and, in some cases, the prodrug structures (**9a-c** and **11a-c**) were used as ligands for the molecular docking.

For all structures, all permutations of stereochemistry (*E/Z* with respect to the oxime) and protonation states (of the oxime and the phosphate moieties – including both stereoisomers for asymmetric protonation) were generated. These structures were optimized at the ω B97xD/6-31+G(2d,p) level prior to molecular docking. In each case, the permutation of the structure resulting in the lowest (best) binding energy was retained as the best binding complex. For rigid docking all residues in the receptor were inflexible while the ligand conformation was explored. For flexible docking the specified flexible residues were for 1QOL (ASP150, SER151, GLU152, SER222, ASN227, LYS228, GLU231, TRP212); 2EGH (ASP149, SER150, GLU151, SER221, ASN226, LYS227, GLU230, TRP211); 3AUA and 3AU9 (ASP231, SER232, GLU233, SER306, ASN311, LYS312, GLU315, TRP296) and for the PfDXR homology model (ASP160, SER161, GLU162, SER235, ASN240, LYS241, GLU244, TRP225). Molecular docking using Autodock 4.2²³ utilized 100 parallel Lamarckian Genetic Algorithm runs, for a maximum of 4500000 calculations together with a maximum of 27000 generations, with a population size of 150. The crossover rate was 0.8 and the mutation rate was 0.02. For the flexible receptor Autodock Vina⁴² and QuickVina-W⁴⁶ were both used for a search area of 22Å around the active site, with the exhaustiveness set to 512. For rigid docking Autodock Vina⁴ was used and the exhaustiveness was set to 512. Visualization was effected in BIOVIA Discovery Studio Visualizer version 17.12.10.⁴⁹

Acknowledgements

The authors thank Rhodes University for a bursary (to M.K.M.), the South African Medical Research Council (MRC) and Rhodes University for generous financial support, and the Centre for High Performance Computing (CHPC project CHEM0802) at the University of Cape Town for computational time.

Supplementary Material

Supplementary material related to this article, including Nuclear Magnetic Resonance (¹H and ¹³C NMR) and in silico docking data are available in the online version of the text.

References

1. World Health Organisation (WHO) *World Malaria Report 2018*. ISBN: 978 92 4 156565 3.
2. Greenwood B. M.; Bojang K., Whitty C. J. M.; Targett G. A. T. *The Lancet* **2005**, *365*, 1487-1498.
[https://doi.org/10.1016/S0140-6736\(05\)66420-3](https://doi.org/10.1016/S0140-6736(05)66420-3)
3. Trig P. I. ; Kondrachine A. V., *The Current Global Malaria Situation*. In *Malaria, Parasite Biology, Pathogenesis, and Protection*; Sherman, I. W., Ed., American Society for Microbiology: Washington, DC, 1998, pp 11-21.
4. Hemingway J.; Ranson H. *Annu. Rev. Entomol.* **2000**, *45*, 371-391.
<https://doi.org/10.1146/annurev.ento.45.1.37>
5. French N.; Nakiyingi J.; Lugada E.; Watera C.; Whitworth J. A. G.; Gilks C. F. *AIDS* **2001**, *15*, 899-906.
<https://doi.org/10.1097/00002030-200105040-00010>

6. Whitworth J.; Morgan D.; Quigley M.; Mayanja B.; Eotu H.; Omoding N.; Okongo M.; Malamba S.; Ojwiya A. *The Lancet* **2000**, 356, 1051-1056.
[https://doi.org/10.1016/s0140-6736\(05\)71332-5](https://doi.org/10.1016/s0140-6736(05)71332-5) PMID: 11213125
7. Van Geertruyden J. P.; D'Alessandro U. *Trends in Parasitology* **2007**, 23, 465-467.
<https://doi.org/10.1016/j.pt.2007.08.006>
8. Milhous W. K.; Kyle D. E. *Introduction to the Modes of Action of and Mechanisms of Resistance to Antimalarials*. In *Malaria, Parasite Biology, Pathogenesis, and Protection*; Sherman, I. W., Ed.; American Society for Microbiology: Washington, DC, 1998, pp. 303-311.
9. Nosten F.; White N. J. *Am. J. Trop. Med. Hyg.*, **2007**, 77, 181-192.
<https://doi.org/10.4269/ajtmh.2007.77.181>
10. Singh N.; Cheve G.; Avery M. A.; McCurdy C. R. *Curr. Pharm. Des.* **2007**, 13, 1161-1177.
<https://doi.org/10.1016/j.ejmech.2007.01.024>
11. Wiesner J.; Jomaa H. *Curr. Drug Targets* **2007**, 8, 3-13.
<https://doi.org/10.2174/13894500777931551>
12. Cassera M. B.; Gozzo F. C.; D'Alexandri F. L.; Merino E. F.; del Portillo H. A.; Peres V. J.; Almeida I. C.; Eberlin M. N.; Wunderlich G.; Wiesner J.; Jomaa H.; Kimura E. A.; Katzin A. M. *J. Biol. Chem.* **2004**, 279, 51749-51759.
<https://doi.org/10.1074/jbc.M408360200>
13. Wiesner J.; Borrmann S.; Jomaa, H. *Parasitol. Res.* **2003**, 90, S71-S76.
<https://doi.org/10.1007/s00436-002-0770-9>
14. Devreux V.; Wiesner, J.; Van Der Eycken J.; Jomaa, H.; Van Calenbergh S. *Bioorg. Med. Chem. Lett.* **2007**, 17, 4920-4923.
<https://doi.org/10.1016/j.bmcl.2007.06>
15. Adeyemi, C. M.; Faridoo; Isaacs, M.; Mnkandhla, D.; Hoppe, H. C.; Krause, R. W. M.; Kaye, P. T. *Bioorg. Med. Chem.* **2016**, 24, 6131-6138, and references cited therein
<https://doi.org/10.1016/j.bmc.2016.04.021>
16. Adeyemi, C. M.; Klein, R.; Isaacs, M.; Mnkandhla, D.; Hoppe, H. C.; Krause, R. W. M.; Kaye, P. T. *Tetrahedron* **2017**, 73, 1661-1667.
<https://doi.org/10.1016/j.tet.2017.01.045>
17. Adeyemi, C. M.; Hoppe, H. C.; Isaacs, M.; Klein, R.; Lobb, K. A.; Kaye, P. T. *Tetrahedron* **2019**, 75, 2371-2378.
<https://doi.org/10.1016/j.tet.2019.02.003>
18. Adeyemi, C.M.; Conibear, A.C.; Mutorwa, M.K.; Nokalipa, I.; Isaacs, M.; Mnkandhla, D.; Hoppe, H.C.; Lobb, K.A.; Klein, R.; Kaye, P.T. *Bioorg. Chem.* In press. (Volume 101 August 2020 Article 103947)
<https://doi.org/10.1016/j.bioorg.2020.103947>
19. Devreux V.; Wiesner, J.; Jomaa, H.; Rozenski J.; Van Der Eycken J.; Van Calenbergh S. *J. Org. Chem.* **2007**, 72, 3783-3789.
<https://doi.org/10.1021/jo0700981>
20. Devreux V.; Wiesner J.; Goeman J. L.; Van Der Eycken J.; Jomaa, H.; Van Calenbergh S. *J. Med. Chem.* **2006**, 49, 2656-2660.
<https://doi.org/10.1021/jm051177c>
21. Verbrugghen T.; Cos P.; Maes L.; Van Calenbergh S. *J. Med. Chem.* **2010**, 53, 5342-5346.
<https://doi.org/10.1021/jm100211e>
22. Mutorwa, M.K. PhD thesis, Rhodes University, 2011.

23. Morris, G. M.; Huey, R.; Lindstrom, W.; Sanner, M. F.; Belew, R. K.; Goodsell, D. S.; Olson, A. J. *J. Comput. Chem.* **2009**, *16*, 2785-91.
<https://doi.org/10.1002/jcc.21256>
24. Yajima S.; Hara K.; Lino D.; Sasaki Y.; Kuzuyama T.; Ohsawa K.; Seto H. *Acta. Crystallogr. Sect. F: Struct. Biol. Cryst. Comm.* **2007**, *63*, 466-470.
<https://doi.org/10.1107/S1744309107024475>
25. Belen'kii L. I.; Kim T. G.; Suslov I. A.; Chuvylkin N. D. *Arkivoc* **2003**, (xiii), 59-67.
<https://doi.org/10.3998/ark.5550190.0004.d08>
26. Kutney J. P.; Hanssen H. W.; Nair G. V. *Tetrahedron* **1971**, *27*, 3323-3330.
[https://doi.org/10.1016/S0040-4020\(01\)97744-0](https://doi.org/10.1016/S0040-4020(01)97744-0)
27. Thomas A. D.; Asokan J.; Asokan C. V.; *Tetrahedron* **2004**, *60*, 5069-5076.
<https://doi.org/10.1016/j.tet.2004.04.017>
28. Rai L. M. K.; Musad E. A.; Jagadish R. L.; Shivakumar K. N. *Synth. Commun.* **2011**, *41*, 953-955.
<https://doi.org/10.1080/00397911003707139>
29. Sarvari H. M.; Sharghi H. *Helv. Chim. Acta*, **2005**, *88*, 2282-2287.
<https://doi.org/10.1002/hlca.200590162>
30. Linda P.; Marino G. *Tetrahedron* **1967**, *23*, 1739-1743.
[https://doi.org/10.1016/S0040-4020\(01\)82573-4](https://doi.org/10.1016/S0040-4020(01)82573-4)
31. Ciranni G. *Tetrahedron Lett.* **1971**, *41*, 3833-3836.
[https://doi.org/10.1016/S0040-4039\(01\)97301-0](https://doi.org/10.1016/S0040-4039(01)97301-0)
32. Hartough H. D.; Kosak A. I. *J. Am. Chem. Soc.* **1947**, *69*, 1012.
<https://doi.org/10.1021/ja01197a010>
33. For the acetylation of the furan derivative **5**, acetic anhydride was used as the acylating agent, rather than acetyl chloride, since a weaker acid (AcOH) is liberated during the reaction and better reaction yields have been reported by Clementi S.; Linda P.; Vergoni M. *Tetrahedron* **1971**, *27*, 4667-4672
[https://doi.org/10.1016/S0040-4020\(01\)98173-6](https://doi.org/10.1016/S0040-4020(01)98173-6)
34. Stumpp M. C.; Schmidt R. R. *Tetrahedron* **1986**, *42*, 5941-5948.
[https://doi.org/10.1016/S0040-4020\(01\)96076-4](https://doi.org/10.1016/S0040-4020(01)96076-4)
35. Pragnacharyulu P. V.; Abushanab E., *Tetrahedron Lett.* **1995**, *36*, 5507-5510.
[https://doi.org/10.1016/00404-0399\(50\)1117Z-](https://doi.org/10.1016/00404-0399(50)1117Z-)
36. Nguyen C.; Kasinathan G.; Leal-Cortijo I.; Musso-Buendia A.; Kaiser M.; Brun R.; Ruiz-Pérez L. M.; Johansson N. G.; González-Pacanowska D.; Gilbert I. H. *J. Med. Chem.* **2005**, *48*, 5942-5954.
<https://doi.org/10.1021/jm050111e>
37. Srinivas O.; Radhika S.; Bandaru N. M.; Nadimpalli S. K.; Jayaraman N. *Org. Biomol. Chem.* **2005**, *3*, 4252-4257.
<https://doi.org/10.1039/b506348e>
38. Ren R. X.; Ou W. *Tetrahedron Lett.* **2001**, *42*, 8445-8446.
[https://doi.org/10.1016/S0040-4039\(01\)01851-2](https://doi.org/10.1016/S0040-4039(01)01851-2)
39. Damljanovic I.; Vukicevic M.; Vukicevic R. D. *Monatsh. Fur. Chem.* **2006**, *137*, 301-305.
<https://doi.org/10.1007/s00706-005-0427-3>
40. Kad G.L.; Bhandari M.; Kaur J.; Rathee R.; Singh J. *Green Chem.* **2001**, *3*, 275.
<https://doi.org/10.1039/b107356g>
41. Kizil M.; Murphy J. A. *Tetrahedron* **1997**, *53*, 16847.
[https://doi.org/10.1016/S0040-4020\(97\)90251-9](https://doi.org/10.1016/S0040-4020(97)90251-9)

42. Trott, O.; Olson, A. J. *J. Comput. Chem.* **2010**, *31*, 455-461.
43. Goble, J. L.; Adendorff, M. R.; de Beer, T. A. P.; Stephens, L. L.; Blatch, G. L. *Protein Pept. Lett.* **2010**, *17*, 109-120.
<https://doi.org/10.2174/092986610789909548>
44. Umeda, T. Tanaka, N., Kusakabe, Y., Nakanishi, M., Kitade, Y.; Nakamura, K.T. *Sci. Rep.* 2011, *1*, 9.
<https://doi.org/10.1038/srep00009>
45. Mac Sweeney, A., Lange, R., Fernandes, R.P., Schulz, H., Dale, G.E., Douangamath, A., Proteau, P.J.; Oefner, C. *J. Mol. Biol.*, 2005, *345*, 115-127.
<https://doi.org/10.1016/j.jmb.2004.10.030>
46. Hassan, N.M.; Alhossary, A.A.; Mu, Y.; Kwoh, C-K., *Sci. Rep.* 2017, *7*, 15451.
<https://doi.org/10.1038/s41598-017-15571-7>
47. Goble J.L.; Johnson, H.; de Ridder, J.; Stephens, I.L.; Louw, A.; Blatch, G.L.; Boshoff, A. *Protein Pept Lett.* = **2013**, *20*, 115-124.
<https://doi.org/10.2174/092986613804725253>
48. Tanner D. C. MSc. Thesis, Rhodes University, Grahamstown, 2003.
49. SYSTÈMES, D. (2016). BIOVIA Discovery Studio *Dassault Syst mes BIOVIA, Discovery Studio Modeling Environment, Release 2017*. Dassault Syst mes

This paper is an open access article distributed under the terms of the Creative Commons Attribution (CC BY) license (<http://creativecommons.org/licenses/by/4.0/>)